

A CLOSED-FORM EXPRESSION APPROXIMATING THE MIE SOLUTION FOR THE REAL-IN-LINE TRANSMISSION OF CERAMICS WITH SPHERICAL INCLUSIONS OR PORES

#WILLI PABST, JAN HOSTAŠA

Department of Glass and Ceramics, Institute of Chemical Technology, Prague, Technická 5, 166 28 Prague, Czech Republic

#E-mail: Willi.Pabst@vscht.cz

Submitted March 4, 2013; accepted June, 16, 2013

Keywords: Optical properties, YAG ceramics (porosity, pore size), YAG-alumina composites, Real-in-line transmission (RIT), Mie solutions and approximations (Rayleigh, Fraunhofer, van de Hulst), Apetz-van-Bruggen approach

A new closed-form expression is presented for estimating the real-in-line transmission of ceramics consisting of non-absorbing phases in dependence of the inclusion or pore size. The classic approximations to the exact Mie solution of the scattering problem for spheres are recalled (Rayleigh, Fraunhofer, Rayleigh-Gans-Debye/RGD, van de Hulst), and it is recalled that the large-size variant of the RGD approximation is the basis of the Apetz-van-Bruggen approach. All approximations and our closed-form expression are compared mutually and vis-a-vis the exact Mie solution. A parametric study is performed for monochromatic light in the visible range (600 nm) for two model systems corresponding to composites of yttrium aluminum garnet (YAG, refractive index 1.832) with spherical alumina inclusions (refractive index 1.767), and to porous YAG ceramics with spherical pores (refractive index 1). It is shown that for the YAG-alumina composites to achieve maximum transmission with inclusion volume fractions of 1 % (and slab thickness 1 mm), inclusion sizes of up to 100 nm can be tolerated, while pore sizes of 100 nm will be completely detrimental for porosities as low as 0.1 %. While the van-de-Hulst approximation is excellent for small phase contrast and low concentration of inclusions, it fails for principal reasons for small inclusion or pore sizes. Our closed-form expression, while less precise in the aforementioned special case, is always the safer choice and performs better in most cases of practical interest, including high phase contrasts and high concentrations of inclusions or pores.

INTRODUCTION

Concomitantly with the development of transparent ceramics for optical windows and ceramic laser materials the question of their optical properties such as the transmittance of visible light and other electromagnetic radiation has become extremely urgent. The literature in this field has grown immensely during the last few years [1-10], but one of the most popular approaches in the last decade has been without doubt the approach proposed by Apetz and van Bruggen [1]. This approach has been used – in its original or more or less modified form – by many authors, although it seems that frequently the assumptions made in this approach are not fully realized. Therefore, in passing, we will comment upon the Apetz-van-Bruggen approach within a concise survey on scattering theory. However, it is not the aim of the present work to review the different attempts of modeling, simulation and experimental efforts in this field. On the contrary, in this paper we will recall some fundamental relations, give a few critical comments on currently used approaches and propose a new pragmatic solution to a question of utmost practical

importance: what relation should be used in practice to roughly estimate the microstructural requirements for achieving transparency, i.e. maximum real-in-line transmittance, in two-phase ceramic composites and in porous ceramics, without making recourse to the exact Mie solution. Based on two well-known and very simple approximations (the Rayleigh and the Fraunhofer approximation), a simple closed-form expression will be proposed that approximates the exact Mie solution for the scattering of spheres. This closed-form expression, which will be tested in a parametric study, can be used in order to estimate the inclusion or pore size dependence of the real-in-line transmittance for different (sufficiently low) inclusion or pore volume fractions. It will be shown that our approach is in special cases slightly less precise than the almost forgotten – albeit extremely interesting and remarkable – van-de-Hulst approximation, but works reasonably well even in cases where the latter fails. Moreover, it will be shown that both the van-de-Hulst approximation and our closed-form expression are of more general validity than the widely used Apetz-van-Bruggen approach.

THEORETICAL

The transmission or transmittance of a material can be defined as the ratio of the intensity (irradiance) of transmitted light I to the intensity of incident light I_0 , multiplied by the theoretical limit of the transmission T_{max} (which principally depends on the optical properties of the material, i.e. on an appropriate average of the complex refractive indices of all phases in the material, and the medium surrounding the macroscopic body), i.e.

$$T = T_{max} \frac{I}{I_0} . \quad (1)$$

However, a real-in-line transmission (RIT) is measured only when the detector angle is small enough (0.5° or smaller [1, 7]). The theoretical limit of the real-in-line transmission (RIT) T_{max} of a non-absorbing material in vacuum or air, i.e. the complement of the total reflection loss R_{total} , is given by

$$T_{max} = 1 - R_{total} = \frac{2n}{1+n^2} , \quad (2)$$

where n is the refractive index. This relation is a consequence of the Fresnel reflectance for normal incidence and specular reflection [1, 11, 12], which for one reflection (on one surface) is

$$R = \left(\frac{n-1}{n+1} \right)^2 , \quad (3)$$

and for multiple reflection (total reflection loss) [1, 7]

$$R_{total} = \frac{2R}{1+R} . \quad (4)$$

Another, completely equivalent, formulation of the theoretical limit of the RIT can be deduced as a special case of the averaged (over interference bands) transmittance through a slab of thickness h [11]

$$T_{max \text{ with absorption}} = \frac{(1-R)^2 \exp(-\alpha_{abs} h)}{1-R^2 \exp(-2\alpha_{abs} h)} , \quad (5)$$

where α_{abs} is the absorption coefficient

$$\alpha_{abs} = \frac{4\pi\kappa}{\lambda} , \quad (6)$$

and κ the absorption index [12], i.e. the imaginary part of the complex refractive index. For small absorption coefficients the series expansions of the exponentials can be cut off before the first-order terms and thus reduce to unity, and the resulting equation is

$$T_{max} = \frac{(1-R)^2}{1-R^2} . \quad (7)$$

This relation, Equation 7, is completely equivalent to Equation 2 above. A very rough (and unnecessary) approximation of this relation is $T_{max} \approx (1-R)^2$, proposed e.g. in [12], and the corresponding approximation for absorbing media in [11]. Needless to say, that these rough approximations have to be avoided.

During transmission, the intensity (irradiance) of light is attenuated not only by reflection (at the surfaces of the macroscopic sample) but also by attenuation (extinction) of the “primary beam“ inside the material. In a strictly homogeneous medium attenuation or extinction inside the material is exclusively due to absorption [11]. However, in heterogeneous materials the intensity (irradiance) is attenuated also by scattering at the heterogeneities, e.g. the inclusion or pores. That means, light is irradiated in directions different from that of the primary beam and thus lost for the RIT. The irradiance entering the material is attenuated according to the Lambert-Beer relation

$$I = I_0 \exp(-\alpha_{ext} h) , \quad (8)$$

as the incident beam traverses the slab of material with heterogeneities, e.g. inclusions or pores. The attenuation or extinction coefficient is

$$\alpha_{ext} = NC_{ext} = NC_{abs} + NC_{sca} , \quad (9)$$

where N is the number of inclusions or pores per unit volume and C_{ext} , C_{abs} and C_{sca} their extinction, absorption and scattering cross sections, respectively. This result can be generalized to a mixture of different particles [11]. However, underlying the exponential attenuation of irradiance in particulate media is the requirement that $\alpha_{ext} h \ll 1$, or at least $NC_{sca} h \ll 1$ (i.e. negligibly small scattering contribution to the total attenuation, see the theory of heat transfer). Strictly speaking, only in this case multiple scattering can be ignored [11]. It is common practice, however, to use this exponential relation beyond its strict range of validity.

The volume fraction ϕ of inclusions or pores is related to the number of inclusions or pores per unit volume N via the relation

$$\phi = N \cdot V_i , \quad (10)$$

where V_i is the volume of a single inclusion or pore. For example, for spherical inclusions or pores one has

$$V_i = \frac{4}{3} \pi r^3 = \frac{\pi}{6} d^3 , \quad (11)$$

(where r is the radius and d the diameter of the sphere), so that for non-absorbing inclusions or pores, where the extinction is only due to scattering, one obtains the attenuation coefficient (= extinction coefficient = scattering coefficient)

$$\alpha_{ext} = \frac{6\phi}{\pi d^3} C_{sca} . \quad (12)$$

Now from Equation 9 above it is clear that the absorption and scattering cross sections are additive, i.e. [11]

$$C_{ext} = C_{abs} + C_{sca} . \quad (13)$$

The fact that the extinction depends only on the scattering amplitude in the forward direction, whereas it is at the same time the combined effect of absorption in

the particle and scattering by the particle in all directions, is a special form of the so-called “optical theorem” [13]. In a similar way, the dimensionless efficiency factors, also called “efficiencies”, defined as

$$Q_{ext} = \frac{C_{ext}}{G}, \quad Q_{abs} = \frac{C_{abs}}{G}, \quad Q_{sca} = \frac{C_{sca}}{G}, \quad (14)$$

where G is the geometric cross section, i.e. the particle cross-sectional area projected onto a plane perpendicular to the incident beam (e.g. $G = \pi r^2 = \pi d^2/4$ for spheres), are additive. Efficiencies are dimensionless cross sections, which can be larger (or smaller) than expected on the basis of geometrical optics: particles can scatter and absorb more light than is geometrically incident on them (according to geometrical optics incident rays are either absorbed or deflected by reflection and refraction) [11]. In terms of efficiencies the attenuation coefficient for a material with nonabsorbing spherical inclusions or pores of one size attains its simplest form:

$$\alpha_{ext} = \frac{3\phi}{2d} Q_{sca}. \quad (15)$$

Inserting this expression into the Lambert-Beer relation and combining the latter with the expression for the theoretical limit of the RIT according to Equation 1, the transmission (transmittance) of a material with spherical inclusions or pores can be calculated, as soon as the efficiency factor for a single inclusion is known. This factor depends on the size of the inclusion or pore (here assumed to be of spherical shape) in relation to the wavelength of light, its optical properties (i.e. in general the complex refractive index, but here assumed to be real, because the inclusions are assumed to be nonabsorbing) and the refractive index of the surrounding medium (usually assumed to be real), i.e. the matrix around the inclusion or pore (usually assumed to be nonabsorbing). Additionally, of course, the grain size dependence of the matrix can be taken into account via the Apetz-van-Bruggen approach [1].

The most convenient dimensionless size parameter commonly used is

$$x = \frac{2\pi nr}{\lambda_0} = \frac{\pi nd}{\lambda} = \frac{\pi d}{\lambda}, \quad (16)$$

where λ_0 is the wavelength of the light in vacuum (or air or another gas) while λ is the wavelength in the material (solid or another condensed matter, e.g. liquid). Also a dimensionless relative refractive index is defined as

$$m = \frac{n_i}{n}, \quad (17)$$

where n_i is the refractive index of the inclusion or pore (here assumed to be real, but generally complex if absorbing) and n the refractive index (usually assumed to be real) of the matrix (nonabsorbing).

When the size of the inclusions or pores is much smaller than the wavelength of light (in the surrounding

matrix), i.e. $x \ll 1$, the efficiency factor is given by the expression for Rayleigh scattering [14],

$$Q_{sca} = \frac{8}{3} x^4 \left(\frac{m^2 - 1}{m^2 + 2} \right)^2. \quad (18)$$

(in the case of complex m the brackets should be replaced by vertical lines indicating real values, and – in addition to scattering efficiencies – absorption efficiencies must be considered as well). It should be recalled that the dimensionless ratio m (relative refractive index) can be smaller than 1, e.g. in the case of pores, while the “dimensionless cross section” Q_{sca} should of course always be a positive quantity. Two extreme cases of this relation are thinkable: for very large m (e.g. water droplets in air at very large wavelengths, where m approaches a value of 9) the efficiency factor approaches the value

$$Q_{sca} = \frac{8}{3} x^4, \quad (19)$$

whereas for m close to 1 the asymptotic value is [14]

$$Q_{sca} = \frac{32}{27} x^4 (m - 1)^2. \quad (20)$$

Another very simple case occurs when the inclusions or pores are very large, i.e. $x \gg 1$. In this case (Fraunhofer diffraction) we have more or less complete forward scattering and the efficiency factor approaches a constant value (in the limit of geometric ray optics) which is

$$Q_{sca} = 2. \quad (21)$$

The fact that the asymptotic value of Q_{sca} for very large x is 2, and not 1, is called the extinction paradox. A plausible explanation of this paradox is given in [14]. For inclusion or pore sizes in the order of the wavelength $d \approx \lambda$, Mie theory should be used [11, 14]. However, even for the simplest shapes, viz. spheres, the exact Mie solution cannot be written down in a few passages and its application requires numerical solution algorithms. Fortunately, these algorithms and user-friendly programs for Mie calculations are available today, e.g. in the form of interactive web applications [15]. Therefore, all approximate solutions may readily be tested vis-à-vis the exact Mie solution. Note that the Rayleigh and Fraunhofer approximations (and of course also the geometric ray optics) do not pose any restrictions on the refractive indices. Both should approach the exact Mie solution for very small and large inclusions or pores, respectively, but are expected to deviate from the Mie solution for inclusion or pore sizes in the vicinity of the wavelength. However, when the relative refractive index is close to 1, i.e. $|m - 1| \ll 1$ and the phase shift is small as well $2x \cdot |m - 1| \ll 1$ [14], recourse can be made to another approximation, the so-called Rayleigh-Gans-Debye (RGD) approximation, which may be a good approximation for inclusion or pore sizes too large for the

Rayleigh approximation. Within the RGD approximation the scattering efficiency can be written as

$$Q_{sca} = (m-1)^2 \cdot \varphi(x) = (m-1)^2 \cdot \left[\frac{5}{2} + 2x^2 - \frac{\sin 4x}{4x} - \frac{7}{16x^2} (1 - \cos 4x) + \left(\frac{1}{2x^2} - 2 \right) \cdot \{0.577... + \log 4x - Ci(4x)\} \right] \quad (22)$$

In this formula the numerical value 0.577... is the Euler constant and $C_i(\dots)$ denotes the so-called cosine integral, see [14], where numerical values of Q_{sca} are tabulated in dependence of the dimensional size parameter x . For $x \ll 1$ the special case of Rayleigh scattering is regained (see Equation 20 above),

$$Q_{sca} = \frac{32}{27} x^4 (m-1)^2, \quad (23)$$

while in the limiting case $x \gg 1$ the scattering efficiency in the RGD approximation is [14]

$$Q_{sca} = 2x^2 (m-1)^2 \quad (24)$$

It has to be recalled that in all correct applications of the RGD approximation the condition

$$Q_{sca} \ll 1 \quad (25)$$

must be fulfilled, because of the requirement of small phase shifts [14], see above. This imposes severe practical restrictions to the usefulness of the RGD approximation for large inclusions or pores (if the refractive index difference is too high) and explains why the RGD approximation cannot be extended into the Fraunhofer region and the region of geometric ray optics, where Q_{sca} approaches a value of 2. The special case of the RGD approximation for large sizes (Equation 24) has been proposed as the basis for calculating the grain size dependence of scattering and transmission in single-phase polycrystalline ceramics (alumina) [1]. However, this calculation according to the Apetz-van-Bruggen approach can only be used when the refractive index difference (in this case the birefringence) is extremely small. In fact, Apetz and van Bruggen used this approach in combination with a very specific (and of course completely virtual) type of effective medium model: they modeled the grain size dependence of transmission by considering the single-phase polycrystalline alumina as if it were a matrix-inclusion-type composite (what it is not) with a refractive index difference of $\Delta n = 0.005$, i.e. for which the matrix has an index of 1.760 and the inclusions an index of 1.765. The idea behind this is that the refractive index difference of this (purely hypothetical) “composite“ should be something like an “orientationally averaged“ birefringence of the crystallites, which is $\Delta n = (2/3)\Delta n_{max}$, where Δn_{max} is the birefringence, i.e. the refractive index difference between the refractive index of the ordinary ray (1.760) and that of the extraordinary ray (1.768). When the shape of the

inclusions is assumed to be spherical (for which there is no justification in this case of course) and the volume fraction of spherical inclusions is assumed to be 0.5 (for which there is also no justification in this case) then we obtain the Apetz-van-Bruggen model. When all these assumptions are accepted, we obtain for 600 nm light a range of validity of the Apetz-van-Bruggen model in the size range (diameter range) of approximately 1 - 25 μm (when the theoretical requirements $x \gg 1$ and $Q_{sca} \ll 1$ are to be fulfilled by a safety factor of ten, i.e. by an order of magnitude) or 0.2 - 50 μm (when the theoretical requirements $x \gg 1$ and $Q_{sca} \ll 1$ are to be fulfilled only by a safety factor of two). It has to be emphasized, however, that alumina (corundum) is a crystal with a rather small birefringence. As soon as the birefringence is higher, e.g. in zirconia at least 0.023 [8] the situation is much more critical (and it has to be noted that much higher birefringence values are reported for zirconia in the literature as well [8]). The range of validity of the Apetz-van-Bruggen model (i.e. the “large sphere variant“ of the RGD approximation) is approximately 0.9 - 5 μm or 0.2 - 8 μm for safety factors of ten and two, respectively. In the case of two-phase composites with alumina inclusions (1.767) in a YAG matrix (1.832), with 50 vol. % of either phase, the validity of the Apetz-van-Bruggen model would be restricted to the very narrow range of 1 - 1.5 μm or 0.2 - 4 μm for safety factors of ten and two, respectively. In other words, in this case the model would be practically useless.

To summarize, the scattering coefficients for the Rayleigh approximation, Fraunhofer (or geometric optics) approximation and the two variants (for small and large spheres) of the RGD approximation are:

- Rayleigh: $\alpha_{Rayleigh} = \frac{4\phi\pi^4 n_m d^3}{\lambda_0^4} \left(\frac{m^2 - 1}{m^2 + 2} \right)^2, \quad (26)$

- Fraunhofer (and geometrical optics): $\alpha_{Fraunhofer} = \frac{3\phi}{d}, \quad (27)$

- RGD (large sphere): $\alpha_{RGD \text{ large}} = \frac{3\phi\pi^2 \Delta n^2 d}{\lambda_0^2}, \quad (28)$

- RGD (small sphere): $\alpha_{RGD \text{ small}} = \frac{16\phi\pi^4 \Delta n^2 n_m^2 d^3}{9\lambda_0^4}. \quad (29)$

With respect to the fact that the calculation of the cosine integral in Equation 22 requires numerical integration and the theoretical requirement $Q_{sca} \ll 1$ generally restricts the use of the RGD approximation anyway (not only its small- and large-sphere variants), there is hardly any advantage – compared to the full exact Mie solution – in using the RGD approximation for spherical inclusions or pores (for non-spherical objects the situation is principally different, simply because a complete Mie solution is not available). However, for very small and very large spheres the Rayleigh approximation and the Fraunhofer (and geometric optics) approximation retain their validity, and an interpolative

combination of these two might be used for roughly estimating the intermediate size range in the vicinity of the wavelength of light without direct recourse to the full Mie solution. For this purpose we propose the following procedure (“R-scaling“, i.e. scaling of the Rayleigh approximation):

- First, calculate the real-in-line transmittance (RIT) according to the Rayleigh approximation, T_R , then according to the Fraunhofer (geometric optics) approximation, T_F .
- Second, cut the Fraunhofer approximation at the vacuum wavelength, rescale the Rayleigh approximation with respect to the RIT at this point and connect the two curves.

The resulting closed-form expression for the relative RIT is then

$$\frac{T}{T_{\max}} = \left[1 - \left(1 - T_R(d) \cdot \frac{1 - T_F(d = \lambda_0)}{1 - T_R(d = \lambda_0)} \right) \right] \cdot T_R(d) + H_{\lambda_0}(d) \cdot T_F(d), \quad (30)$$

where $H_{\lambda_0}(d)$ is the Heaviside step function defined as

$$H_{\lambda_0}(d) = \begin{cases} 0 & \text{for } d < \lambda_0 \\ 1 & \text{for } d \geq \lambda_0 \end{cases} \quad (31)$$

Of course, the choice of $d = \lambda_0$ is to a certain degree arbitrary and by adapting this cutoff value the fit to the Mie solution could be optimized. A simpler alternative, albeit much rougher as an approximation to the Mie solution, would be the use of the maximum function:

$$\frac{T}{T_{\max}} = \max(T_R(d), T_F(d)) \quad (32)$$

In the following sections we will compare our closed-form expression, Equation 30, and the simple maximum function, Equation 32, to the exact Mie solution and the aforementioned approximations (Rayleigh, RGD, Fraunhofer), as well as another approximation, which is extremely useful, but has been largely neglected in the literature so far: the van de Hulst approximation (vdH approximation). Within this approximation, which holds for non-absorbing spheres, the scattering efficiency can be written in the form [14]

$$Q_{sca} = 2 - \frac{4}{\rho} \sin \rho + \frac{4}{\rho^2} (1 - \cos \rho) \quad (33)$$

with

$$\rho = 2x(m - 1) \quad (34)$$

In contrast to the RGD approximation, which performs well only for relative refractive indices close to unity ($m \rightarrow 1$), the vdH approximation works well even for values of m as large as 2 [14] and is indeed one of the most useful and precise approximations to the Mie solution.

RESULTS AND DISCUSSION

Parametric study

Figure 1 shows the theoretical maximum transmittance of materials calculated according to Equations 2 or 7. The bold region indicated in the central part of this curve refers to typical oxides, the refractive index of which is practically always in the range 1.4 - 2.7 (at wavelengths of visible light). The theoretical maximum transmittance corresponding to this range of refractive indices is in the range 65.1 - 94.6 % for optically homogeneous materials. Heterogeneities such as second-phase inclusions, pores and (in the case of non-isotropic crystallites also) grain boundaries reduce the transmittance. Of course, since the refractive index depends on the wavelength, also the maximum transmittance changes with the wavelength.

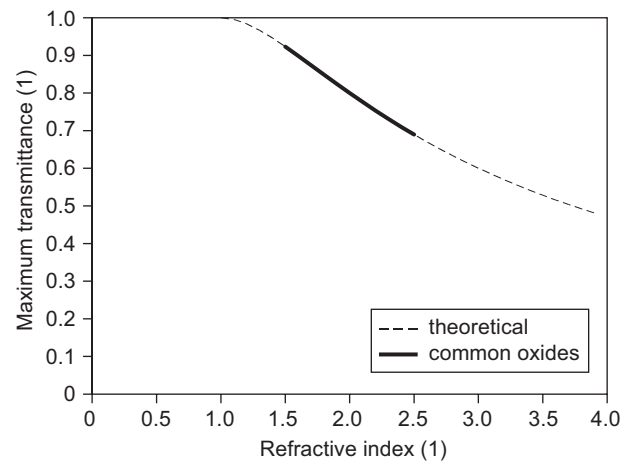


Figure 1. Theoretical maximum transmittance of typical oxides at visible wavelengths.

For a wavelength of 600 nm, which is somewhere in the middle of the visible range, the refractive index of yttrium-aluminum garnet (YAG = $Y_3Al_5O_{12}$) is $n = 1.832$ [16], while alumina ($\alpha-Al_2O_3$) has at this wavelength refractive indices $n_o = n_{\perp} = 1.7702$ and $n_e = n_{\parallel} = 1.7618$, respectively [17], i.e. exhibits a birefringence of -0.0084 . Using the mixture rule

$$\varepsilon = \frac{\varepsilon_{\parallel} + 2\varepsilon_{\perp}}{3} \quad (35)$$

for the dielectric permittivity of an isotropic polycrystalline aggregate of uniaxial crystallites, we obtain the arithmetic average refractive index as

$$n = \sqrt{\frac{n_{\parallel}^2 + 2n_{\perp}^2}{3}} \quad (36)$$

For alumina at 600 nm this value is 1.767. Thus the refractive indices of YAG and alumina are relatively close. In fact, the difference between the two ($\Delta n \approx 0.065$) is very similar to the difference of the

refractive indices of the ordinary and extraordinary rays ($\Delta n = n_o - n_e$) of tetragonal zirconia, which is reported to be in the range 0.023 - 0.093 [8, 18, 19]. Therefore, since the Apetz-van-Bruggen approach, which is based on the RGD approximation (large sphere variant), has been successfully used to model the grain size dependence of the RIT of tetragonal zirconia [8], it would seem even more appropriate to apply the RGD approximation for YAG-alumina composites, because in contrast to the modeling of the grain size dependence of the RIT via the Apetz-van-Bruggen approach, where the differently oriented crystallites are treated as if they were virtual inclusions, YAG-alumina composites are really two-phase composites and are therefore ideally suited to serve as a playground for parametric studies. Potential

practical aspects of these composites, such as the possible development two-wavelength lasers, will be discussed in a forthcoming paper.

Figures 2a-d show the scattering patterns of a model system containing spherical inclusions with refractive index 1.767 in a matrix with index 1.832, according to Mie calculations for a wavelength of 600 nm, using Scott Prah's web-based "Mie Scattering Calculator" [15]. This model system can be considered as representative for YAG-alumina composites with low volume fractions of randomly oriented alumina inclusions in visible light. In these so-called "polar graphs" of the scattering pattern, light is incident from the left on a sphere located at the center. The radial axis in these graphs possesses a linear scale. Although the intensity of scattered light

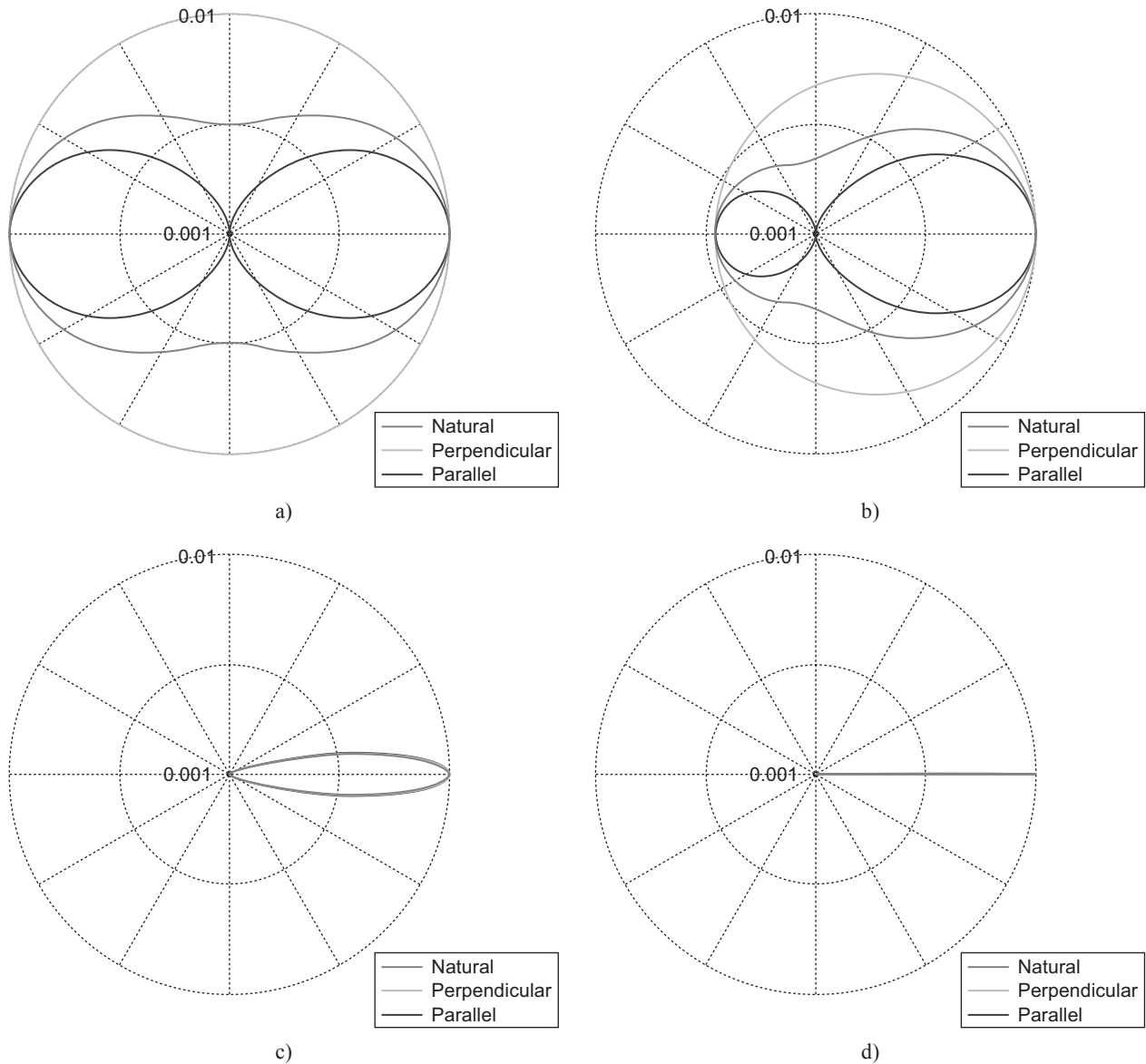


Figure 2. Scattering patterns of a (nonabsorbing) spherical inclusion with diameter 0.01, 0.1, 1, 10 μm (Figures 2a, 2b, 2c and 2d, respectively, from top to bottom) and refractive index $n = 1.767$ (alumina) in a (nonabsorbing) matrix with $n = 1.832$ (YAG) in monochromatic light in the visible range $\lambda = 600 \text{ nm}$; polar graph with linear radial axes.

is shown for the cases of incident light with parallel and perpendicular polarization as well, only the case of natural light (circumscribed figures) is of interest to us here. Figures 3a-d show similar scattering patterns of a model system containing spherical inclusions with refractive index 1 in a matrix with index 1.832, for a wavelength of 600 nm. This system corresponds to porous YAG ceramics at low porosities.

In both cases the scattering patterns are very similar. It is evident that for inclusion diameters smaller than 100 nm there is a considerable amount of scattering in the backward direction (backscattering) and that for 10 nm inclusions the scattering is completely isotropic (Rayleigh limit), whereas for inclusion diameters larger than 1 μm the scattering is essentially in the forward

direction (small-angle scattering, Fraunhofer diffraction and geometric optics limit).

Figures 4 and 5 show the dependence of the scattering efficiency on the size of spherical inclusions or pores for YAG-alumina composites ($n_{\text{matrix}} = 1.832$, $n_{\text{inclusion}} = 1.767$) and porous YAG ceramics ($n_{\text{matrix}} = 1.832$, $n_{\text{pore}} = 1$), respectively. In the first case, the phase contrast is sufficiently close to unity (i.e. the difference between the two refractive indices is sufficiently small) for the (two variants of the) Rayleigh-Gans-Debye (RGD) approximation to be justified, in the second case it is not. However, for reasons of comparison, the RGD approximations have been calculated also for this case and are shown in Figure 5.

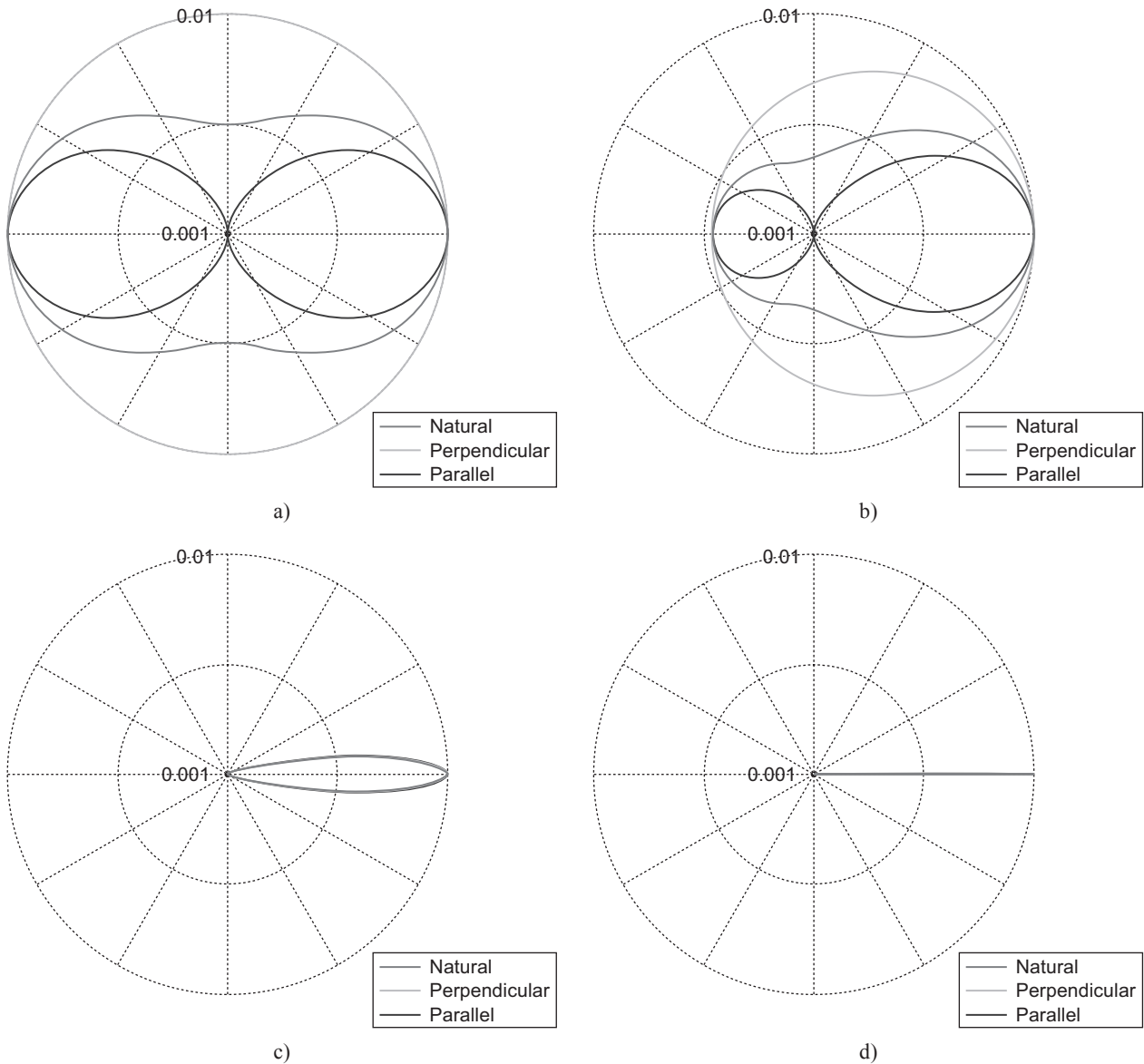


Figure 3. Scattering pattern of a spherical pore inclusion with diameter 0.01, 0.1, 1, 10 μm (Figures 3a, 3b, 3c and 3d, respectively, from top to bottom) in a (nonabsorbing) matrix with $n = 1.832$ (YAG) for monochromatic light in the visible range ($\lambda = 600$ nm); polar graph with linear radial axes.

Figure 4 shows that the vdH approximation is an excellent approximation to the exact Mie solution for YAG-alumina composites at 600 nm, far better than any other approximation. The vdH approximation is an initially increasing and subsequently oscillating function which decreasing amplitude that levels off to the Fraunhofer diffraction limit value of the scattering efficiency of two ($\lim_{Q \rightarrow \infty} Q = 2$). With decreasing inclusion size the vdH approximation approaches the large-size variant of the RGD approximation from below

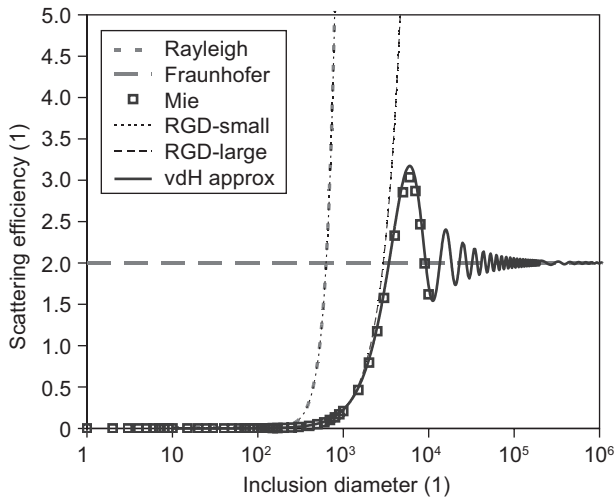


Figure 4. Dependence of the scattering efficiency on the size of spherical inclusions for YAG-alumina composites in monochromatic light at 600 nm, calculated according to the Rayleigh approximation, the Fraunhofer approximation, the two variants of the Rayleigh-Gans-Debye (RGD) approximation, the van-de-Hulst approximation (vdH) and the exact Mie theory.

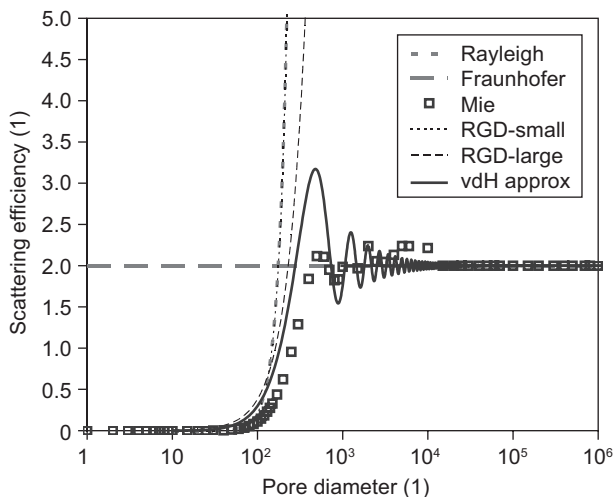


Figure 5. Dependence of the scattering efficiency on the size of spherical pores for porous YAG ceramics in monochromatic light at 600 nm, calculated according to the Rayleigh approximation, the Fraunhofer approximation, the two variants of the Rayleigh-Gans-Debye (RGD) approximation (unjustified in this case), the van-de-Hulst (vdH) approximation and the exact Mie theory.

and remains below the small-size variant of RGD approximation down to an inclusion diameter of approx. 135 nm. Below this size, the scattering efficiency of the vdH approximation (and also the large-size variant of the RGD approximation) exceeds the small-size variant of RGD approximation and becomes thus unrealistic.

Figure 5 refers to the case of porous YAG ceramics. In this case, where the small-size RGD approximation is shifted to smaller values and the large-size RGD approximation is closer to the small-size RGD, it is evident that the vdH approximation is not as good as before, but seems not to be much worse than the other approximations. However, also in this case its validity is restricted to pore diameters larger than approx. 135 nm, and it will be shown that this failure has serious consequences when either the phase contrast or the inclusion concentration are large.

Figures 6 through 8 show the inclusion size dependence of the real-in-line transmission (RIT) of YAG-based composite ceramics (matrix: YAG $n = 1.832$ – inclusion: alumina $n = 1.767$) in monochromatic light of wavelength ($\lambda = 600$ nm) for alumina (inclusion) volume fractions of 0.1, 1 and 10 %, respectively, calculated (for a slab thickness 1 mm) according to different models, including our closed-form expression (denoted “R-scaling”), the van-de-Hulst (vdH) approximation and the exact Mie solution. It is evident, that for inclusion volume fractions as low as 0.1 % the vdH approximation is by far the best approximation to the Mie solution. However, already for an inclusion volume fraction of 1 % the RIT prediction calculated using the vdH approximation is highly misleading. It would lead to the conclusion that

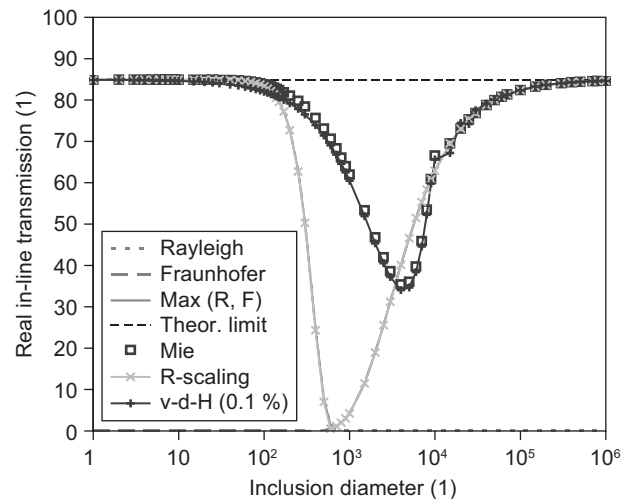


Figure 6. Inclusion size dependence of the real-in-line transmission of YAG-based composite ceramics (matrix: YAG $n = 1.832$ – inclusion: alumina $n = 1.767$) for monochromatic light in the visible range ($\lambda = 600$ nm) for an alumina (inclusion) volume fraction of 0.1 % and a slab thickness of 1 mm, calculated according to different models, including our closed-form expression (R-scaling), the van-de-Hulst (v-d-H) approximation and the exact Mie solution.

inclusion sizes considerably smaller than 10 nm would be necessary to achieve maximum RIT, whereas in reality (according to the Rayleigh approximation and the exact Mie solution) inclusion sizes of several tens of nm would be appropriate, which appears much more feasible to realize in practice. For inclusion volume fractions

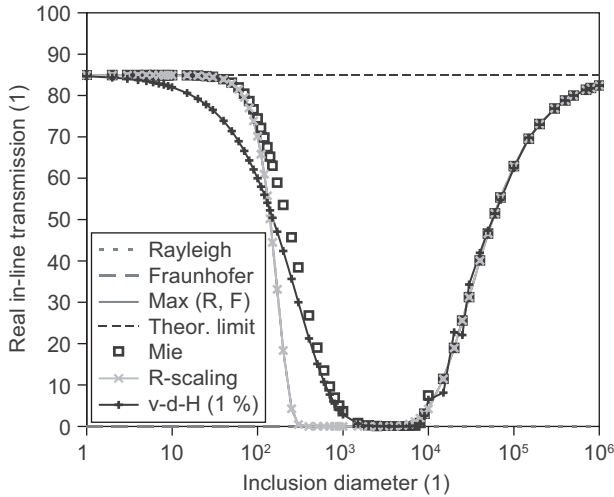


Figure 7. Inclusion size dependence of the real-in-line transmission of YAG-based composite ceramics (matrix: YAG $n = 1.832$ – inclusion: alumina $n = 1.767$) for monochromatic light in the visible range ($\lambda = 600$ nm) for an alumina (inclusion) volume fraction of 1 % and a slab thickness of 1 mm, calculated according to different models, including our closed-form expression (R-scaling), the van-de-Hulst (v-d-H) approximation and the exact Mie solution.

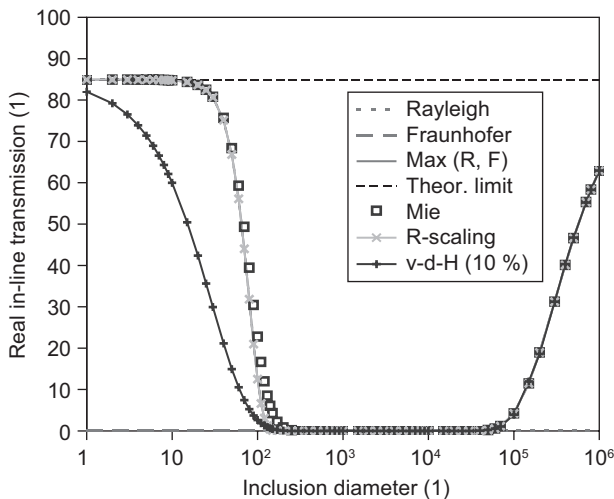


Figure 8. Inclusion size dependence of the real-in-line transmission of YAG-based composite ceramics (matrix: YAG $n = 1.832$ – inclusion: alumina $n = 1.767$) for monochromatic light in the visible range ($\lambda = 600$ nm) for an alumina (inclusion) volume fraction of 10 % and a slab thickness of 1 mm, calculated according to different models, including our closed-form expression (R-scaling), the van-de-Hulst (v-d-H) approximation and the exact Mie solution.

of 10 % the vdH approximation fails completely for inclusion sizes smaller than approx. 200 nm, while our closed-form expression is almost as good as the exact Mie solution.

Figures 9 through 14 show the pore size dependence of the real-in-line transmission (RIT) of porous YAG ceramics ($n = 1.832$) for monochromatic light in the visible range ($\lambda = 600$ nm) for porosities of 0.0001, 0.001, 0.01, 0.1, 1 and 10 % and a slab thickness of 1 mm according to exact Mie theory, the Rayleigh approximation, the Fraunhofer approximation, the vdH approximation and our closed-form expression (R-scaling).

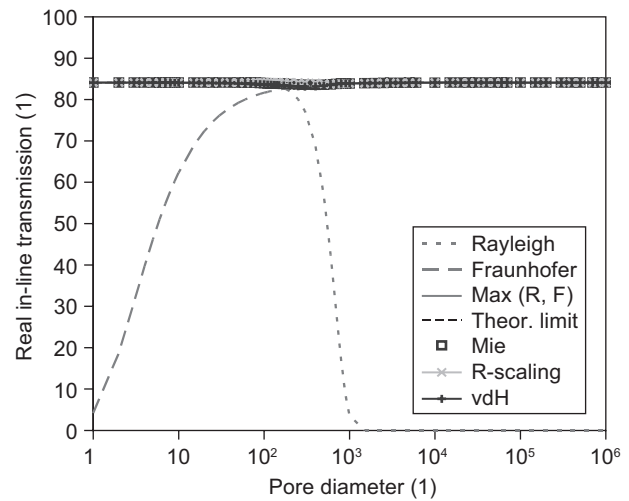


Figure 9. Pore size dependence of the real-in-line transmission of YAG ceramics ($n = 1.832$) for monochromatic light in the visible range ($\lambda = 600$ nm) for a porosity of 0.0001 % and a slab thickness of 1 mm according to exact Mie theory and several approximations, including our closed-form expression.

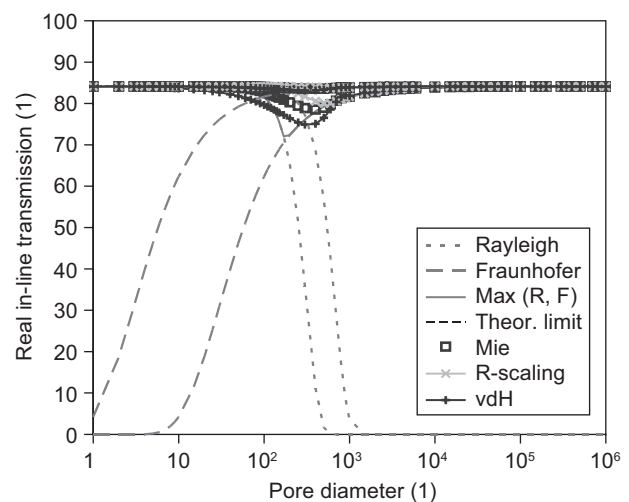


Figure 10. Pore size dependence of the real-in-line transmission of YAG ceramics ($n = 1.832$) for monochromatic light in the visible range ($\lambda = 600$ nm) for a porosity of 0.001 % and a slab thickness of 1 mm according to exact Mie theory and several approximations, including our closed-form expression.

It is evident that porosities of the order 0.0001 % have virtually no influence on the RIT, see Figure 9. However, already porosities as low as 0.001 % lead to a sensible decrease of the RIT when the pore size is critical, i.e. similar to the wavelength of light, see Figure 10. For this case, where the phase contrast is high (the ratio of the two refractive indices is 1.832), the vdH approximation predicts a RIT that is too low and comes to lie even below the Rayleigh approximation for pore diameters smaller than 135 nm, which is clearly unrealistic. On the other hand, our close-form expression provides values

that are slightly higher than the exact Mie solution, but approach the Rayleigh approximation for small pore size, as required on physical grounds. For porosities of order 0.1 % and higher the material becomes more or less opaque when the pore size is submicron (i.e. pore diameters of several hundred nm), and for porosities of order 1 % and higher the pore size should be of order 10 nm and lower to attain maximum RIT. With increasing porosity from 0.01 to 10 % the vdH becomes more and more unrealistic, whereas our closed-form expression more and more approaches the exact Mie solution.

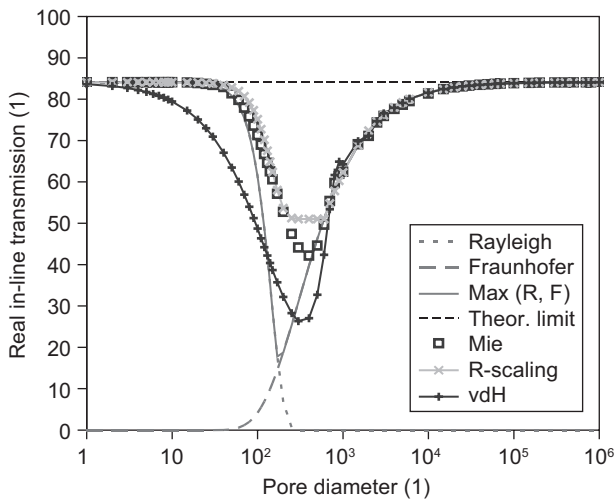


Figure 11. Pore size dependence of the real-in-line transmission of YAG ceramics ($n = 1.832$) for monochromatic light in the visible range ($\lambda = 600$ nm) for a porosity of 0.01 % and a slab thickness of 1 mm according to exact Mie theory and several approximations, including our closed-form expression.

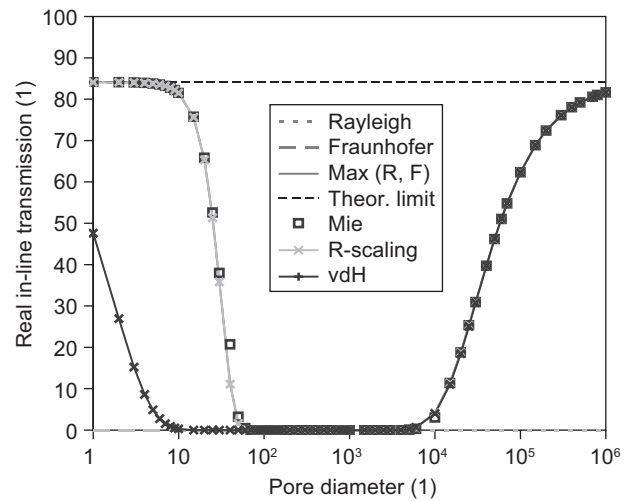


Figure 13. Pore size dependence of the real-in-line transmission of YAG ceramics ($n = 1.832$) for monochromatic light in the visible range ($\lambda = 600$ nm) for a porosity of 1 % and a slab thickness of 1 mm according to exact Mie theory and several approximations, including our closed-form expression.

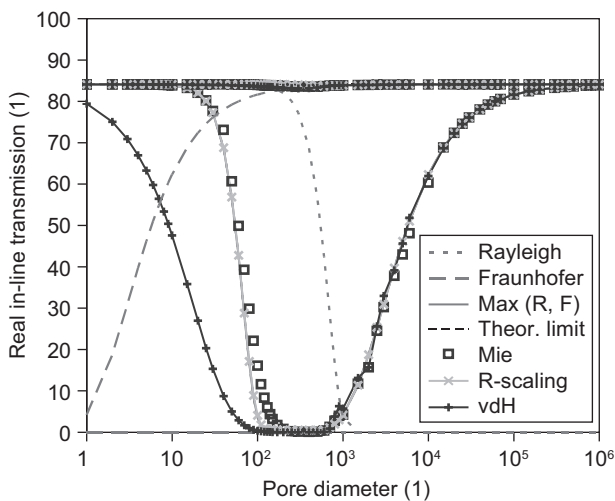


Figure 12. Pore size dependence of the real-in-line transmission of YAG ceramics ($n = 1.832$) for monochromatic light in the visible range ($\lambda = 600$ nm) for a porosity of 0.1 % and a slab thickness of 1 mm according to exact Mie theory and several approximations, including our closed-form expression.

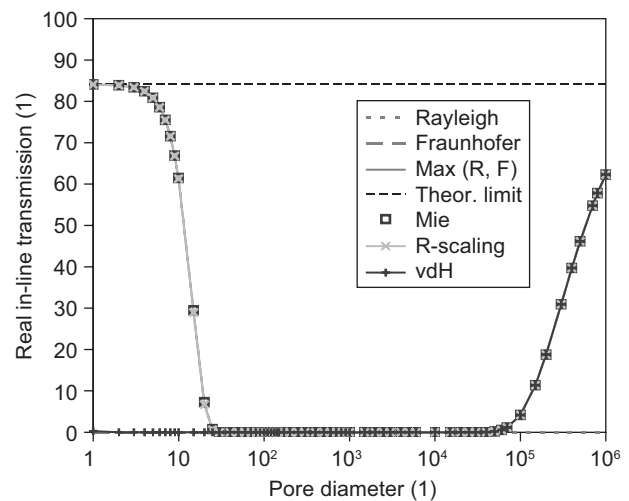


Figure 14. Pore size dependence of the real-in-line transmission of YAG ceramics ($n = 1.832$) for monochromatic light in the visible range ($\lambda = 600$ nm) for a porosity of 10 % and a slab thickness of 1 mm according to exact Mie theory and several approximations, including our closed-form expression.

SUMMARY AND CONCLUSIONS

A new closed-form expression has been presented that enables one to estimate the real-in-line transmission of ceramics consisting of non-absorbing phases, e.g. of certain composites or porous ceramics, in dependence of the inclusion or pore size. In the theoretical part of this paper the classic approximations to the exact Mie solution of the scattering problem for spheres have been recalled (Rayleigh, Fraunhofer, Rayleigh-Gans-Debye / RGD) and commented upon. In particular, it has been emphasized that there are two variants of the RGD approximation (small-size and large-size variant) and that the latter is – together with other, very specific assumptions – the basis of the popular Apetz-van-Bruggen approach, which is briefly criticized in passing. Moreover, in the theoretical part another – less well known, but all the more useful – approximation has been brought to light from the shadows of oblivion: the van de Hulst approximation. The latter relation and our simple closed-form expression (essentially a combination of the Rayleigh and Fraunhofer approximations) have been compared mutually and vis-a-vis the exact Mie solution. A parametric study has been performed for monochromatic light in the visible range (600 nm) for two model systems corresponding to composites of yttrium-aluminum garnet (YAG, matrix with refractive index 1.832), and alumina (spherical inclusions with refractive index 1.767) and to porous YAG ceramics with spherical pores (refractive index 1). The parametric study has shown that for the YAG-alumina composites to achieve maximum transmission with inclusion volume fractions of 1 % (and slab thickness 1 mm), inclusion sizes of up to 100 nm can be tolerated, while pore sizes of 100 nm will be completely detrimental for porosities as low as 0.1 %. While the van-de-Hulst approximation is excellent for small phase contrast (e.g. here a refractive index difference of 0.065) and low concentration (e.g. 0.1 % of alumina inclusions in a YAG matrix), it fails for principal reasons for small inclusion or pore sizes. Our closed-form expression, while slightly less precise in the aforementioned special case, is always the safer choice and performs definitely better in most cases of practical interest, including high phase contrasts (e.g. here a refractive index difference of 0.832) and high concentrations of inclusions or pores.

Acknowledgements

W.P. acknowledges support from the Czech Science Foundation (GAČR No. P108/12/1170) and J.H. from the Internal Grant Agency (IGA) of the ICT Prague for specific university research (MŠMT No. 20/2013).

REFERENCES

1. Apetz R., van Bruggen M.P.B.: *J. Am. Ceram. Soc.* **86**, 480 (2003).
2. Ikesue A., Kinoshita T., Kamata K., Yoshida K.: *J. Am. Ceram. Soc.* **78**, 1033 (1995).
3. Krell A., Blank P., Ma H., Hutzler T., van Bruggen M. P. B., Apetz R.: *J. Am. Ceram. Soc.* **86**, 12 (2003).
4. Jasbinder S., Kim W., Villalobos G., Shaw B., Baker C., Frantz J., Sadowski B., Aggarwal I.: *Opt. Mater.* **35**, 693 (2013).
5. Ikesue A., Yoshida K., Yamamoto T., Kamata K., Yamaga I.: *J. Am. Ceram. Soc.* **80**, 1517 (1997).
6. Pecharroman C., Mata-Osoro G., Díaz L.A., Torrecillas R., Moya J. S.: *Optics Express* **17**, 6899 (2009).
7. Krell A., Hutzler T., Klimke J.: *J. Eur. Ceram. Soc.* **29**, 207 (2009).
8. Klimke J., Trunec M., Krell A.: *J. Am. Ceram. Soc.* **94**, 1850 (2011).
9. Stuer M., Bowen P., Cantoni M., Pecharroman C., Zhao Z.: *Adv. Funct. Mater.* **22**, 2303 (2012).
10. Zhang W., Lu T., Wei N., Wang Y., Ma B., Li F., Lu Z., Qi J.: *J. Alloys Comp.* **520**, 36 (2012).
11. Bohren C.F., Huffman D.R.: *Absorption and Scattering of Light by Small Particles*, p. 12-165. Wiley, New York 1983 (reprint Wiley-VCH, Weinheim 2004).
12. Kingery W.D., Bowen H.K., Uhlmann D.R.: *Introduction to Ceramics*, second edition, p. 646-703, Wiley, New York 1976.
13. Newton R.G.: *Am. J. Phys.* **44**, 639 (1976).
14. van de Hulst H. C.: *Light Scattering by Small Particles*, p. 63-227. Wiley, New York 1957 (reprint Dover Publications, New York 1981).
15. Prah S.: *Mie Scattering Calculator*, Oregon Medical Laser Center, Portland 2012.
16. Ovanesyan K.L., Petrosyan A.G., Shirinyan G.O., Avetisyan A.A.: *Izv. Akad. Nauk SSSR (Ser. Neorg. Mater.)* **17**, 459 (1981) and *Inorg. Mater.* **17**, 308 (1981).
17. DeFranzo A.C., Pazol B.G.: *Appl. Opt.* **32**, 2224 (1993).
18. Rignanese G.M., Detraux F., Gonze X., Pasquarello A.: *Phys. Rev. B* **64**, 134301 (2001).
19. Garcia J.C., Scolfaro L.M.R., Lino A.T., Freire V.N., Farias G.A., Silva C.C., Leite Alves H.W., Rodrigues S.C.P., da Silva E.F.: *J. Appl. Phys.* **100**, 104103 (2006).